ANTIMICROBIAL AGENTS AND CHEMOTHERAPY, Oct. 2010, p. 4321–4328 Vol. 54, No. 10
0066-4804/10/$12.00 doi:10.1128/AAC.00006-10

Structural Characterization of IS*CR8*, IS*CR22*, and IS*CR23*, Subgroups of IS*91*-Like Insertion Elements[▽]

Kathleen M. Schleinitz,[1]* Tatiana Vallaeys,[2] and Sabine Kleinsteuber[1]

UFZ Centre for Environmental Research Leipzig-Halle, Department of Environmental Microbiology, Permoserstr. 15, 04318 Leipzig, Germany,[1] and Laboratoire ECOLAG, UMR CNRS-UMII 5119, Université Montpellier II, cc 093, Place E. Bataillon, F-34095 Montpellier Cedex 5, France[2]

Received 4 January 2010/Returned for modification 23 April 2010/Accepted 2 July 2010

Analysis of IS*CR8* (IS*Pps1*) revealed that this group of insertion elements has to be subdivided into three subgroups: IS*CR8*, IS*CR22*, and IS*CR23*. The distinction of three subgroups is supported by phylogenetic analysis of the transposase open reading frames (ORFs). Comparison of over 20 complete and partial IS*CR8*/*22*/*23* elements identified *ori*IS candidate sequences for all groups and a *ter*IS candidate sequence for IS*CR8*. The *ori*IS sequences, their distance to the transposase ORFs, and the sequence of this intervening region are group specific, further supporting the definition of two new IS*CR* elements. IS*CR8*/*22*/*23* have a very broad host range, including Gram-positive and Gram-negative bacteria, among which are several (opportunistic) pathogens. The IS often resides on plasmids or in the vicinity of other mobile elements and is mostly associated with genes for the degradation of halo- or nitro-aromatics. However, in one case IS*CR8* was found in the neighborhood of an antibiotic resistance determinant in *Klebsiella pneumoniae*. IS*CR8* resembles other IS91 family elements in mediating genetic rearrangements by homologous recombination between two copies. In *Delftia acidovorans* this led to the loss of the genes encoding dichlorprop cleavage. In conclusion, this study shows that IS*CR8* could be a fully functional and active member of the IS*91* family of insertion elements.

The widespread use of antimicrobial agents in human and veterinary medicine as well as animal husbandry exerts a selective pressure that has led to the emergence of a multitude of resistance mechanisms. Both the emergence of new resistance determinants and their rapid spread throughout microbial communities are of considerable public concern.

Transfer of resistance determinants is frequently mediated by mobile genetic elements, i.e., plasmids, transposons, integrons, and insertion elements (IS elements). Recently, a new group of insertion elements, IS*CR*, was identified (20, 21). IS*CR* is a subgroup of IS*91*-like elements. These are unusual in replicating via the rolling circle mechanism and being bounded by an *ori*IS, the origin of replication, and a *ter*IS, the termination sequence (6, 12, 18). The *ori*IS is indispensable for transposition, and replication always starts at this sequence. Due to aberrant termination, i.e., readthrough of the *ter*IS site, IS*91*-like elements are able to mobilize fragments of DNA adjacent to *ter*IS. This is currently considered the main avenue by which IS*91*-like elements contribute to the dissemination of genes (6). Additionally, they participate in shaping the genetic makeup of their hosts by homologous recombination (22, 23).

The IS*CR* subgroup of IS*91*-like elements currently comprises 21 members (http://medicine.cf.ac.uk/en/research/research-groups/i3/research/antibacterial-agents/iscr-elements/). *In silico* analyses suggested that their insertion, in contrast to that of canonical IS*91* elements (IS*91*, IS*801*, and IS*1294*) (6, 13, 18), is not site specific. The GTTC tetramer found adjacent to the *ori*IS of canonical IS91 elements is not found adjacent to the *ori*IS of IS*CR* elements (21). Another distinguishing feature is the lack of one of the two key amino acid residues (Tyr249 and Tyr253) necessary for transposition of IS*91* elements (6, 13). In IS*CR* elements Tyr249 is replaced by arginine or lysine. This led to the hypothesis that transposition of IS*CR*s proceeds by a mechanism different from that of canonical IS*91* (21).

IS*CR* elements have played an important role in the dissemination of a number of recently identified antimicrobial resistance genes, including extended-spectrum beta-lactamases (reference 3 and literature cited therein). Moreover, they were involved in the evolution of complex integrons bringing together resistance genes that previously were transferred independently (3).

Although IS*CR*s have almost exclusively been found to be associated with resistance determinants (3, 21), there are two exceptions, IS*CR7* and IS*CR8*. IS*CR8* (designation according to ISfinder [16], IS*Pps1*) seems to be primarily associated with genes for the degradation of (halo)aromatics (15, 21). In *Delftia acidovorans* MC1, *rdpA* and *sdpA*, the genes encoding cleavage of the herbicide dichlorprop (2[2,4-dichlorophenoxy]propionate), are flanked and interspersed by IS*CR8* elements (15). Under nonselective conditions, i.e., in the absence of the herbicide, these genes are easily deleted. At the same time, the number of IS*CR8* elements is strongly reduced, suggesting that recombination between copies of IS*CR8* might cause the loss of dichlorprop cleavage.

IS*CR8* elements have not been analyzed in detail. The copy in *Pseudomonas pseudoalcaligenes* JS45 was postulated to be truncated and nonfunctional, as it was supposed to be lacking essential features of active IS*91* elements (21). However, a closer inspection of IS*CR8* in other strains revealed that at least some contain *ori*IS sequences (15) and that, moreover, at least one copy is associated with a beta-lactamase gene. These

* Corresponding author. Mailing address: UFZ Helmholtz Centre for Environmental Research, Dept. of Environmental Microbiology, Permoserstr. 15, 04318 Leipzig, Germany. Phone: 49-341-235-1378. Fax: 49-341-235-1351. E-mail: kathleen.schleinitz@ufz.de.

▽ Published ahead of print on 12 July 2010.

TABLE 1. Primers used in this study

Name	Sequence (5′–3′)[a]	Source
COS-F	AAG CAT TGG TAA CTG TCA G	This study
COS-R	GGA ATG AAC AAT GGA AGT C	This study
FP-1	AGT TCA AGC TTG TCC AGG AAT TC$(N)_7$ GGC CT	17
FP-2	AGT TCA AGC TTG TCC AGG AAT TC$(N)_7$ GCG CT	17
FP-3	AGT TCA AGC TTG TCC AGG AAT TC$(N)_7$ CCG GT	17
FP-4	AGT TCA AGC TTG TCC AGG AAT TC$(N)_7$ CGC GT	17
6aF	ATT GGT CAG GTA CCA AGC	This study
6aR	CGC ACT CAA GAT ACT TGG	This study
IS91outF	CAT CAT TGC CTT CAT CAC C	This study
SdpoutR	TGA CGG TGG CGC CCA GGG TG	This study
ProlipoR	GTT CGC CAT TGA TGA AGT TGC	This study
R10-f	GGT GCG ACA GGT AAT AGC	This study
R10r	ATC TGC GTT AGT TCC TGG	This study
AcylCoAout R	CGG CGA ACT CAA TGT AGC	This study
K-antip_F	AGG GGA GTT GGC AAT GAC C	This study
K-antip_R	CAC GAT CAG CAG GTC TTC G	This study
Dihydroxy_F	GAG GGC GAC TTC AAG AAG C	This study
Dihydroxy_R	GCT TCA GGT CGC AGA TCA CG	This study

[a] $(N)_7$, any nucleotide ($n = 7$).

findings led us to conduct an in-depth analysis of IS*CR8* elements.

MATERIALS AND METHODS

***In silico* structural analysis of IS*CR8*-related elements.** BLAST (1) was used to search for IS*CR8*-like transposase open reading frames (ORFs) in nucleotide and protein sequence databases (GenBank, EMBL, and DDBJ). Inspection of the sequences surrounding the transposase ORFs, including identification of *ori*IS and *ter*IS candidate sequences, was carried out using Vector NTI Advance (InforMax). The deduced amino acid sequences of all IS*CR8*-like transposases were aligned using MultAlign (5) and ClustalW (19). On the basis of these alignments, transposase sequences were screened for deletions, insertions, and rearrangements, and amino acid sequence motifs known to be of functional importance (6) were identified.

Construction of phylogenetic trees. The deduced amino acid sequences of all complete IS*CR8*-like transposases as well as one to five sequences each of IS*91*, IS*801*, IS*1294*, and IS*CR1* to -*7* were aligned using MultAlign. The IS*CR8* transposase of *Comamonas testosteroni* CNB-1 was omitted due to a large duplication within the conserved amino acid sequence motif II (see below). Neighbor-joining and minimum evolution trees were calculated from the resulting 431-amino-acid alignment using MEGA2.1 (10). Poisson correction, *p*-distance, and the number of differences were applied as distance models. Bootstrap analysis was performed based on 1,000 resamplings.

Strains, plasmids, and culture conditions. *Delftia acidovorans* MC1, *D. acidovorans* MC1-DP$^-$ (a mutant of strain MC1 that arose by spontaneous loss of dichlorprop cleavage), and *Escherichia coli* XL-Blue MRF′ (Stratagene) containing the genomic library cloned in cosmid vector pScosPA1 were all maintained or grown as described before (15).

DNA isolation. Plasmid and cosmid DNAs were isolated using a Nucleobond AX100 kit (Macherey-Nagel).

DNA amplification. All primer sequences used for PCR amplifications are listed in Table 1. The ends of five cosmid inserts known to carry *rdpA* but not *sdpA* were amplified using semirandom two-step PCR (ST-PCR) (4). To each sample either the primer COS-F or COS-R, annealing to the ends of the cosmid vector and facing into the insert, was added as specific primer, and either of four FP primers (FP-1 to -4) (17) was added as random primer. All primers were synthesized by MWG Biotech.

Rearrangements of plasmid pMC1 were analyzed by PCR with the following pairs of primers: for PCR-1, 6aF and 6aR, amplifying a 544-bp fragment spanning the left end of IS*CR8* and the region flanking it (see Fig. 5); for PCR-2, IS91outF and SdpoutR, amplifying a 569-bp fragment spanning the right boundary of IS$CR8_L$ and the region flanking it; for PCR-3, ProlipoR and R10_r, amplifying a 611-bp fragment spanning the left boundary of the right duplicated region and the region flanking it; for PCR-4, IS91outF and AcylCoAoutR, amplifying a 575-bp fragment spanning the right boundary of IS$CR8_R$ and the region flanking it.

PCR products for use as hybridization probes were generated as follows: a 451-bp region at the left ends (LE) of the duplicated region was amplified using primers R10_f and R10_r. A 482-bp fragment of an ORF for a putative potassium antiporter (KA) was amplified using primers K_antip_F and K_antip_R. An 838-bp segment of an ORF for a putative dihydroxy acid dehydratase (DH) was amplified using primers Dihydrox_F and Dihydrox_R.

For all PCRs the *Taq* PCR Mastermix kit (Qiagen) and a PTC-200 thermal cycler (MJ Research) were used. The fragments were amplified using a cycling program involving an initial denaturation step at 94°C for 3 min, followed by 35 cycles of 94°C for 45 s, 55°C (PCR-1), 62°C (PCR-2), 59°C (PCR-3), 61°C (PCR-4), 58°C (LE), or 62°C (KA and DH) for 45 s, and 72°C for 1 min, with a final elongation step at 72°C for 6 min.

Sequencing and sequence analysis of a cosmid insert and PCR products were performed as described previously (15).

DNA-DNA hybridization. DNA of plasmids pMC1 and pMC1-DP$^-$ was digested with PstI or EcoRI and XmaI according to standard procedures and separated electrophoretically in 2% agarose gels overnight at 2 V cm^{-1}. Blotting and hybridization were carried out as described previously (15). The hybridization temperatures were 55°C (LE) and 60°C (KA and DH, respectively).

Nucleotide sequence accession numbers. The nucleotide sequences determined in this study were deposited in the GenBank, EMBL, and DDBJ databases as an update of accession number AY327575.

RESULTS AND DISCUSSION

IS*CR8* transposases. BLAST searches with the originally described IS*CR8* transposase gene of *Pseudomonas pseudoalcaligenes* JS45 (accession number AF028594) revealed 15 complete ORFs resembling it, as well as a number of truncated ORFs. Among each other, the IS*CR8*-related transposases shared between 100 and 71% identity, as calculated from the deduced amino acid sequences. The large variation in sequence already indicated that not all of the sequences are true IS*CR8* transposases but that some belonged to one or more new groups of IS*CR* elements. Identities to IS*91*/*801*/*1294* transposases varied between 19 and 32%, and those to other IS*CR* elements ranged between 32 and 34%. These identities were distributed over the entire sequences. The amino acid alignment also showed that the C termini of all IS*CR8*-related transposases are conserved (data not shown), but three sequences displayed prolonged N termini (Fig. 1A). Two of these sequences contained a methionine residue at the position that marks the start of translation in IS*CR8* of strain JS45. The

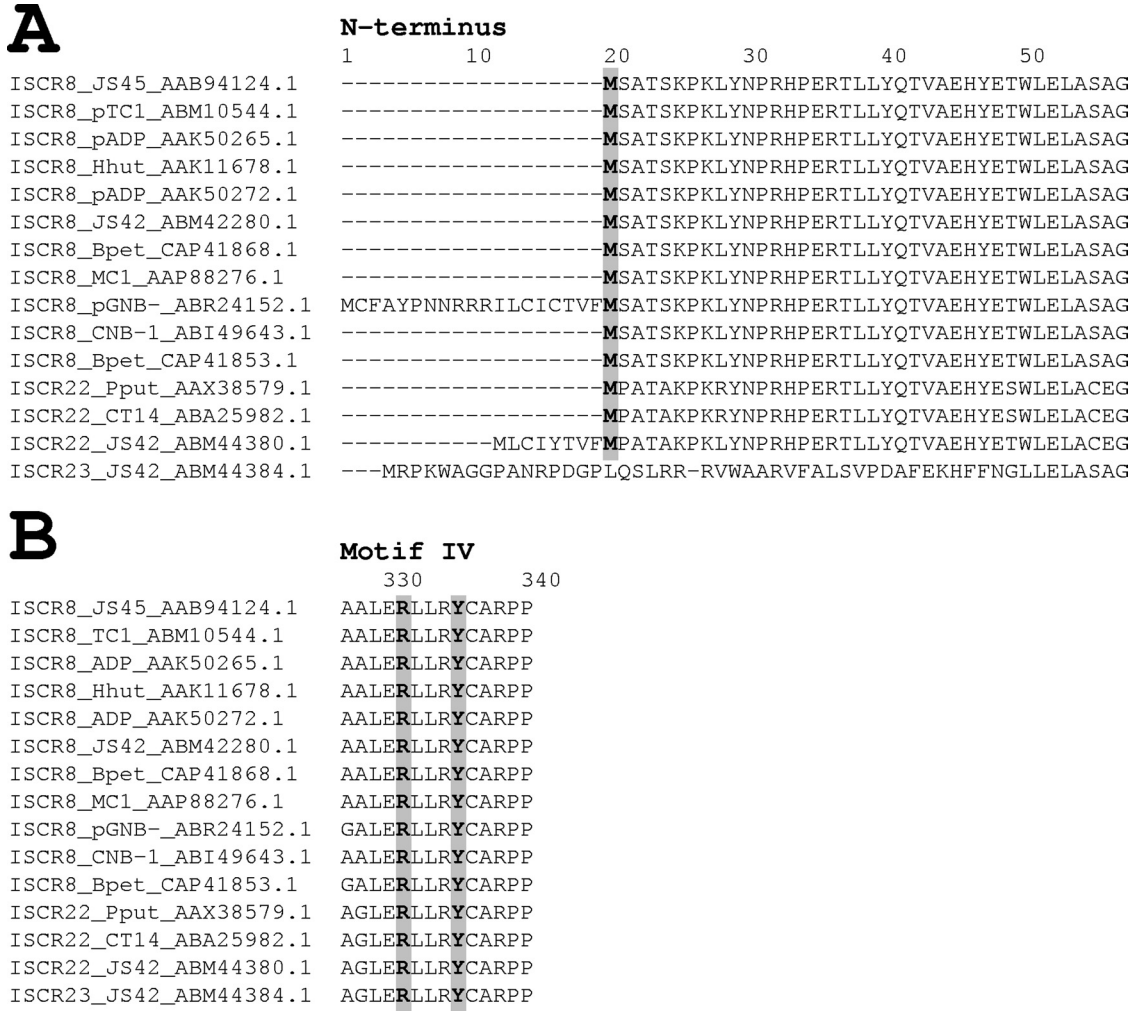

FIG. 1. Partial sequence alignment of IS*CR8*/*22*/*23* transposases. (A) N termini; (B) motif IV, the functional motif that in canonical IS*91* elements contains two tyrosine residues essential for rolling circle transposition. In IS*CR8*/*22*/*23* transposases, one of the tyrosine residues (positions shaded in gray) is replaced by arginine. To the left of the alignment IS*CR* names, strain designations and accession numbers are given. JS45, *Pseudomonas pseudoalcaligenes* JS45; TC1, *Arthrobacter aurescens* TC1 plasmid pTC1; ADP, *Pseudomonas* sp. plasmid pADP-1; Hhut, *Herbaspirillum huttiense*; JS42, *Acidovorax* sp. JS42; Bpet, *Bordetella petrii*; MC1, *Delftia acidovorans* MC1 plasmid pMC1; pGNB, *D. acidovorans* plasmid pGNB1; CNB-1, *Comamonas* sp. plasmid pCNB-1; CT14, *Pseudomonas* sp. plasmid CT14; Pput, *Pseudomonas putida*. The alignment was created using MultAlign.

extended N termini are therefore likely to be artifacts resulting from conceptual translation.

As observed for the originally described IS*CR8* (21), all of the conserved amino acid sequence motifs of IS*91*-like elements (7) are present in the IS*CR8*-related transposases, among them the family signature in motif III (G-X_5-[H/Q]-X-[F/W/Y]-G-X_5-[H/N]-X-H-X-H-X_5-G). However, the tyrosine residue corresponding to the functionally essential Y249 of canonical IS*91* (Y331 in Fig. 1) was replaced by arginine. This is a feature distinguishing and differentiating IS*CR8* from canonical IS*91* elements. The same substitution has already been documented for other IS*CR* elements (21) and led to speculations about a different subunit architecture of IS*CR* transposases compared to canonical IS*91* transposases.

As stated previously (21), it was observed here that IS*CR8*-related transposases contain several insertions and deletions compared to canonical IS*91* family elements. The transposase of *C. testosteroni* CNB-1 contains a 21-amino-acid duplication within motif II that probably renders it inactive. The same would be true for the insertion into the transposase of *Klebsiella pneumoniae*. Alignments of the IS*CR8*-related transposases with canonical IS*91*/*801*/*1294* elements furthermore showed that the former contain a 2-amino-acid insertion and a 1-amino-acid deletion within motif I (data not shown). The same insertion and deletion are also present in other IS*CR* elements (21). All additional insertions and deletions detected in IS*CR8*-like transposases were located outside the conserved motifs. These results show that in most cases the insertions and deletions are in the same range as those discriminating IS*CR1* to *-7* elements from canonical IS*91* elements and do not affect the conserved amino acid sequence motifs. The overall structure of IS*CR8*-related transposases may still be conserved, and therefore functionality may not be affected by these alterations of primary structure.

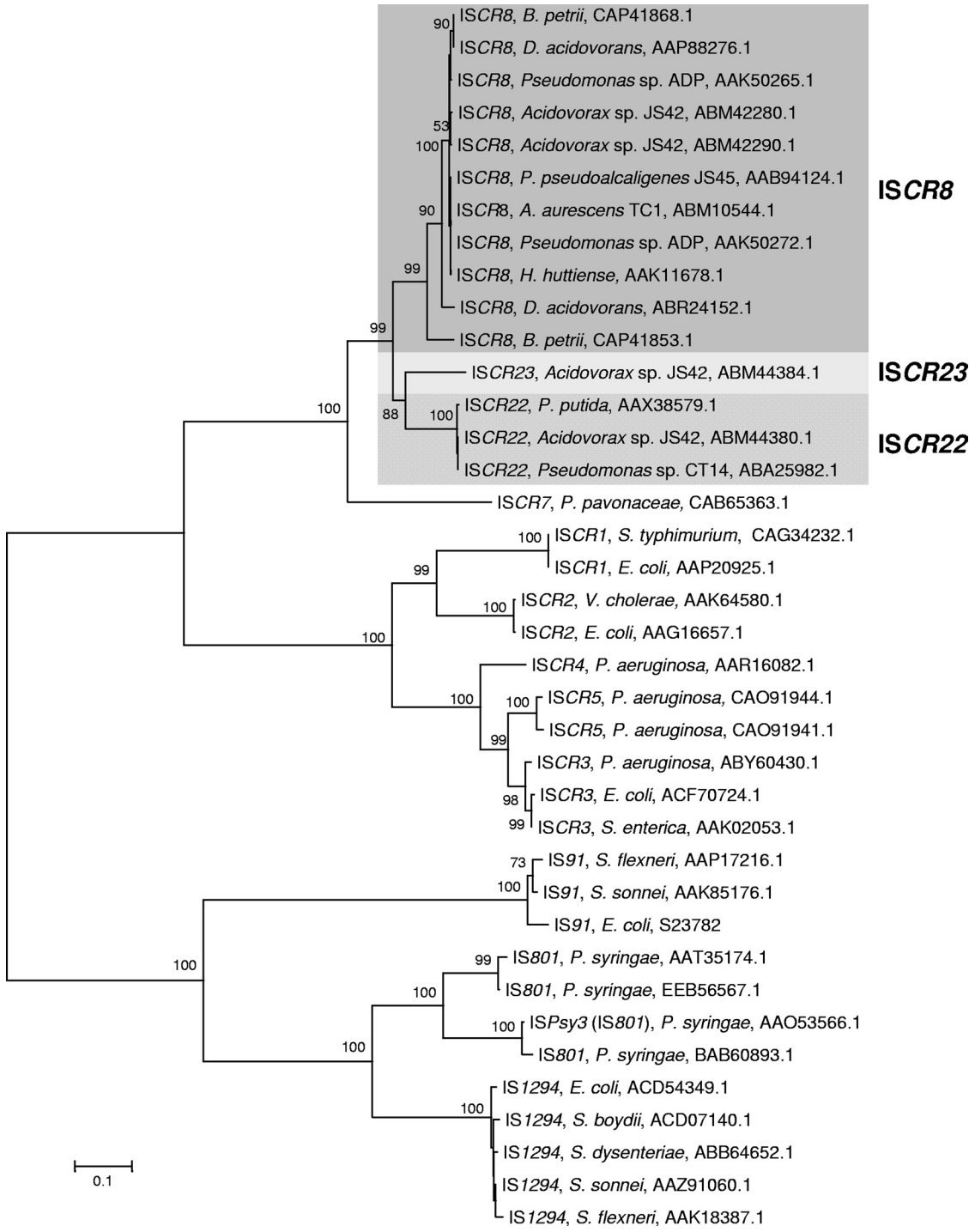

FIG. 2. Phylogenetic tree of IS*91* family transposases. The neighbor-joining tree was inferred from 431 aligned positions of IS*91*, IS*801*, IS*1294*, and IS*CR* transposase sequences. In the case of IS*91*, IS*801*, and IS*1294*, not all sequences available were included, and partial sequences were generally not included. The alignment was computed with MultAlign, and a Poisson distribution was applied as the distance model. Bootstrap analysis was performed based on 1,000 resamplings, and bootstrap values above 50% are indicated at the respective nodes. Bar, an estimate change of 10%.

The phylogenetic relationship of IS*CR8*-related transposases and other IS*91*-like transposases is represented in Fig. 2. Tree topology was robust when different methods for calculation were used, and trees were validated by bootstrap analysis. This held true for the positions of single IS*CR* elements as well as for the IS*CR* subgroup forming a sister group of the canonical IS*91*-like elements. IS*CR8* transposases are most closely related to IS*CR7*, as would be expected from comparison of total

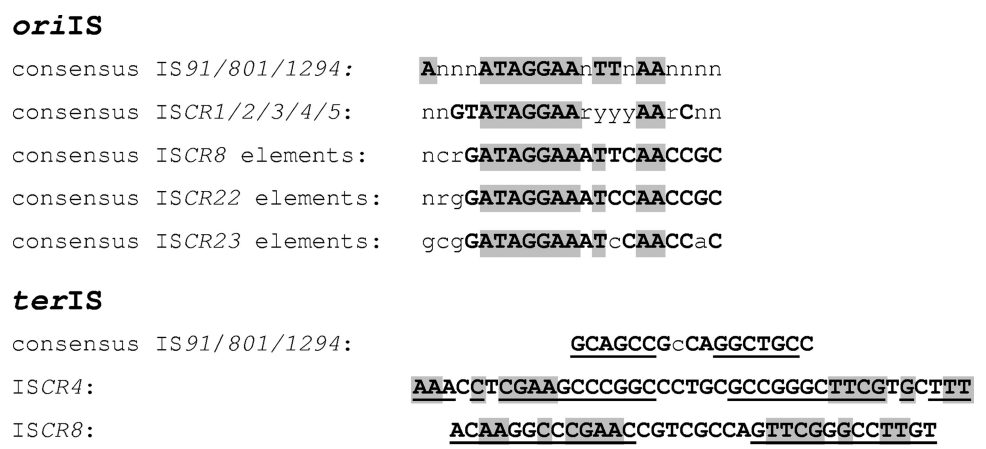

FIG. 3. Comparison of conserved sequences at the end of IS*91*-like elements. (Top) *ori*IS consensus sequence of canonical IS*91*-like elements (18), putative *ori*IS sequences of IS*CR1* to -*5* (20), IS*CR8*, IS*CR22*, and IS*CR23*. (Bottom) *ter*IS consensus sequence of canonical IS*91*-like elements (18), putative *ter*IS of IS*CR4* (20), and IS*CR8*. Nucleotides conserved within a subgroup are indicated by bold, uppercase letters. Nucleotides conserved between subgroups are additionally shaded in gray. Nonconserved nucleotides are shown in lowercase letters. Inverted repeats are underlined. IUPAC ambiguity code: R is A or G, Y is T or C, and N is any nucleotide.

amino acid sequence identities. All IS*CR7*/IS*CR8* elements form a deep-branching clade, showing that they are long diverged members of the IS*CR* subgroup of IS*91* elements. The phylogenetic tree shows that the IS*CR8*-related transposases form three clades. The originally described IS*CR8* of *P. pseudoalcaligenes* belongs to the largest clade, which therefore contains all true IS*CR8*s. IS*CR8* transposases are 515 amino acids long. The second largest clade contains three nearly identical members that are 526 amino acids long and share 78% sequence identity with IS*CR8*. The third cluster contains one sequence of 538 amino acids that is 76% identical to IS*CR8*. The distinction of three clades is not only supported by phylogenetic analysis and the length of the transposases but also mirrored by structural features (see below). We therefore propose two new subgroups of IS*CR* elements, IS*CR22* and IS*CR23* (Fig. 2). It is noteworthy that *Acidovorax* sp. JS42 carries members of all three subgroups: the two transposase genes located on the chromosome belong to IS*CR8*, and those located on the plasmid belong to IS*CR22* and IS*CR23* (Fig. 2; see also Fig. 4, below).

Structural features of IS*91*-like elements in IS*CR8*/IS*CR22*/IS*CR23*. Analysis of the regions flanking the transposase genes revealed a sequence downstream of the transposase ORFs that strongly resembles *ori*IS (Fig. 3). This sequence is present in most of the IS*CR8* copies, including the one originally described (21), with the only exceptions being two truncated IS*CR8* elements of *Pseudomonas putida* plasmid pNB2 and *Comamonas* sp. plasmid pCNB-1, as well as one chromosomal copy of *Acidovorax* sp. JS42 (Fig. 3). All of the nucleotides conserved in the *ori*IS of canonical IS*91* elements are conserved throughout IS*CR8*, with the exception of IS*CR8*s in *D. acidovorans* MC1, *Sphingobium herbicidovorans* MH, and *P. putida* (Fig. 3). This 20-bp sequence is therefore proposed to constitute the *ori*IS of IS*CR8* elements. The distance between *ori*IS and the transposase gene is always 166 bp. Apart from one A-G exchange in *K. pneumoniae*, this stretch of sequence is identical in all IS*CR8* elements.

All IS*CR22* elements were accompanied by an *ori*IS candidate sequence that differed slightly from that of IS*CR8* (Fig. 3). The sequence is conserved throughout all IS*CR22* and was located 176 bp downstream of the transposase ORF. The intervening sequence is identical in all IS*CR22* elements and shows only 53% sequence identity to the respective sequence in IS*CR8*.

An *ori*IS candidate sequence for IS*CR23* was found 161 bp downstream of the transposase ORF. Its sequence differs slightly from those of IS*CR8* and IS*CR22* and is therefore specific for IS*CR23*. The sequences flanking IS*CR8*/*22*/*23* at the putative *ori*IS sites are different for each copy of the elements, further suggesting that the *ori*IS may be functional.

Inspection of the sequence upstream of the transposase genes revealed a 10-bp perfect inverted repeat in some IS*CR8* elements (Fig. 3 and 4). The IR sequence resembles the putative *ter*IS of IS*CR4* and is therefore a candidate sequence for *ter*IS in IS*CR8* elements. The distance of the putative *ter*IS to the start codon of the transposase gene is always 53 bp. Except for one nucleotide these 53 bp are identical in all IS*CR8*. However, unlike the sequence flanking IS*CR8*/*22*/*23* at the putative *ori*IS, the first 36 bp flanking IS*CR8* at the putative *ter*IS are identical. Whether the *ter*IS candidate sequence is not functional or is often misread is not known at the moment.

No *ter*IS candidate sequence was identified in IS*CR22* or IS*CR23*. This is a phenomenon described for other IS*91*-like elements that are often not accompanied by a *ter*IS (7, 12). A *ter*IS is not a prerequisite for functionality of IS*91* elements, because they are capable of one-ended transposition.

As already observed with other IS*CR* elements (21), the tetranucleotide GTTC or CTTG was not found to flank the *ori*IS of IS*CR8* elements. Transposition of canonical IS*91* elements is site specific and takes place at the 5′ end of this tetranucleotide (13). The lack of the tetranucleotide at IS*CR* insertion sites has led to speculation about differences in the transposition mechanism of these elements (24). However, these hypotheses await experimental confirmation.

Genetic context of IS*CR8*/IS*CR22*/IS*CR23*. IS*CR8* elements have a broad host range. As depicted in Fig. 4, they were found

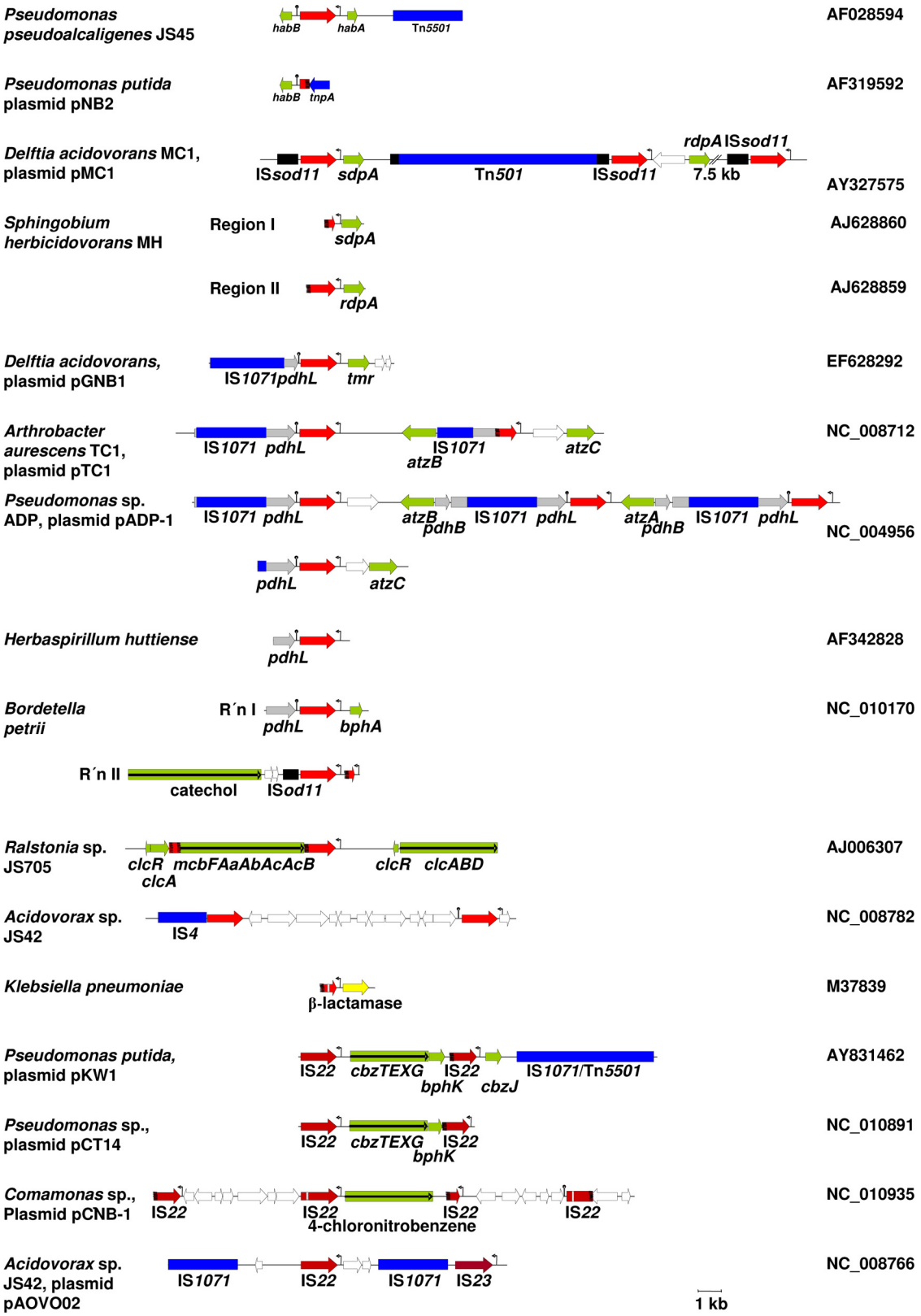

FIG. 4. Genetic context of IS*CR8*/*22*/*23* elements in various host genomes. Color coding of ORFs: red, IS*CR8* transposases (unless stated otherwise); green, genes for degradation of (halo)aromatics; blue, mobile genetic elements other than IS*CR8*; white/gray, other ORFs. Symbols: arrows above ORF, *ori*IS; dot and stalk above ORF, *ter*IS; white box within ORF, insertion; horizontal lines at right or left end of ORF, partial ORF. Gene designations: *habA*/*habB*, hydroxylaminobenzene mutase; *tnpA*, transposase; *sdpA*, *S*-dichlorprop dioxygenase; *rdpA*, *R*-dichlorprop dioxygenase; *pdhL*, dihydrolipoamide dehydrogenase; *pdhB*, dihydrolipoamide acetyltransferase; *tmr*, triphenylmethane reductase; *atzA*/*atzB*/*atzC*, atrazine degradation; *clcR*/*clcABC*, chlorocatechol degradation; *bphA*/*bphK*, biphenyl dioxygenase; *mcbFAaAbAcAcB*, chlorobenzene degradation; *cbzTEXG*, chlorobenzene degradation (*meta*-cleavage pathway).

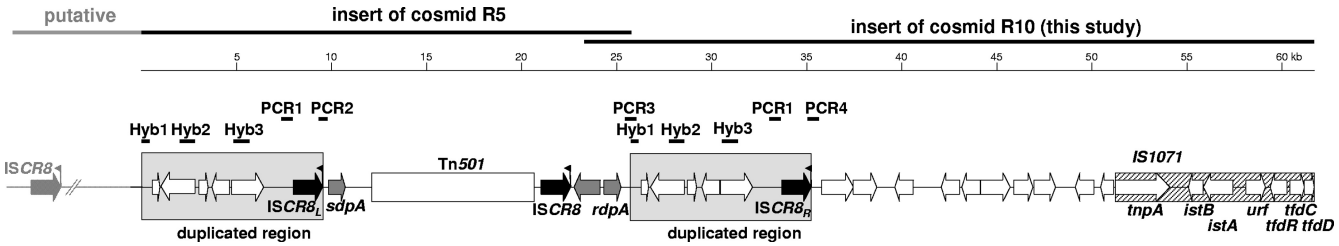

FIG. 5. Rearrangements within *Delftia acidovorans* MC1 plasmid pMC1. In the mutant plasmid pMC1-DP$^-$, an ~40-kb region including the genes for dichlorprop cleavage (*rdpA* and *sdpA*), transposon Tn*501*, and a duplicated region of ~9 kb is deleted, presumably by homologous recombination between two copies of IS*CR8*, as verified by Southern hybridization (Hyb1 to -4 indicate the probes) and PCR (PCR1 to -4 indicate the regions amplified). The outer right boundary of the deletion was identified, but attempts to identify the left boundary failed. Shading of open reading frames: black, upper pathway of dichlorprop degradation; dark gray, IS*CR8* transposase; white, other ORFs. Shading of genetic regions: light gray, duplicated region (99% identical copies); stripes, lower pathway of dichlorprop degradation (99% identity to corresponding regions of other bacteria); white, Tn*501*.

in Gram-negative bacteria (*Alpha-*, *Beta-*, and *Gammaproteobacteria*) as well as Gram-positive bacteria (*Arthrobacter aurescens* TC1). The host range includes several genera of (opportunistic) pathogens. IS*CR8/22/23* elements are often located on plasmids but are also carried by the chromosome of the host. Similarly to other IS*CR* elements they are frequently associated with genes not belonging to the core genome of the host. IS*CR8/22/23* elements are often found in the vicinity of genes for the breakdown of (halo-/nitro-)aromatics, such as chlorobenzene, catechol, or atrazine (for a detailed description see the Fig. 4 legend). However, in one instance IS*CR8* was identified next to a broad-spectrum beta-lactamase gene in *K. pneumoniae* (14) (Fig. 4). The sequence available only covers the 3′ end of the transposase ORF, and therefore it is not known whether the strain carries a complete or a truncated IS*CR8* transposase gene. The deduced amino acid sequence shows highest sequence identity to the IS*CR8* transposases of *Bordetella petrii* and *A. aurescens* TC1. However, an insertion near the 3′ end probably renders the IS*CR8* transposase inactive.

In database searches for IS*91*-like elements, a high proportion of partial copies was detected (7). The same applied to IS*CR8/22*. Various copies, inactivated by truncation of the transposase ORF at the 3′ or 5′ end, were identified. However, IS*91* family transposases act with similar efficiencies in *cis* and in *trans* (2). Therefore, partial copies can be transposed by the gene product of a complete copy somewhere else in the host genome as long as they contain an *ori*IS, part of the sequence stretching from the *ori*IS toward the transposase ORF, and the GTTC tetramer. Whether a partial IS*CR8/22* can be transposed in the same way is not known at the moment. Complete IS*CR8/22* elements were often found in close proximity to truncated homologues and could potentially provide an active transposase. Several of the partial copies contain an *ori*IS and could therefore serve as a target for the transposase. However, as stated above, the GTTC tetramer is missing, and the implications of this for the transposition process are unclear.

Furthermore, the nonrandom distribution of IS*CR8/22* elements within the host genomes is noticeable, i.e., when several copies are present in one strain they are often located near each other. In this aspect the elements studied here seem to resemble IS*91* in *Shigella flexneri* 2457T. In a genome-wide survey investigating the spatial distribution of over 200 insertion sequences in this strain, only IS*91* and IS*911* appeared to be nonrandomly distributed (24). This was explained with local hopping, i.e., the transposition mechanism is biased toward placing new copies near the parent copy, rather than natural selection favoring insertion into particular regions of the genome.

IS*91*-like elements are often found in the neighborhood of other mobile elements, and on plasmids (7). IS*CR1* and IS*CR3* were observed to be primarily associated with complex class 1 integrons (21). Among the mobile elements associated with IS*CR8/22/23*, IS*1071* predominates (Fig. 4 and 5). This is also the case in *Comamonas* sp. plasmid pCNB-1, where four (partial or interrupted) copies of IS*CR8* are located on Tn*CNB1*, an approximately 46-kb composite transposon bordered by two IS*1071* elements (11). Whether IS*1071* aids in the spread of IS*CR8* or vice versa is difficult to judge. In the genome of *Comamonas* sp. CNB-1, Tn*CNB1* would be expected to mediate transposition of IS*CR8*. However, in *Pseudomonas* sp. ADP it appears that a module consisting of IS*CR8*, *pdhL*, IS*1071*, and *pdhB* exists. During one-ended transposition, fragments of variable lengths adjacent to IS*CR8* were replicated, resulting in the transposition of more or less complete copies of this module into different sites on plasmid pADP-1. This view that such a module exists is also supported by the fact that *Herbaspirillum huttiense*, *B. petrii*, and *D. acidovorans* plasmid pGNB1 carry IS*CR8* with flanking *pdhL* genes, and in the case of plasmid pGNB1 this also includes an IS*1071*.

It is intriguing that several subgroups of IS*91*-like elements seem to be associated with a particular group of genes: IS*91* and IS*1294* are primarily associated with pathogenicity determinants in animals, IS*801* is linked to plant pathogenicity determinants, IS*CR* elements other than IS*CR7* and IS*CR8/22/23* are found in the vicinity of antibiotic resistance determinants, and IS*CR8/22/23* are mainly associated with degradative traits. Horizontal gene transfer has clearly played a dominant role in the dissemination of the degradative traits associated with the elements studied here. Although the exact role IS*CR8/22/23* have played in the process is as yet unclear, this is signified by degradative traits being located on plasmids and in the vicinity of various insertion elements or transposons.

Rearrangements caused by IS*CR8* in *D. acidovorans* MC1. In *D. acidovorans* MC1 degradation of the herbicide dichlorprop is initiated by two dioxygenases, RdpA and SdpA. Loss of the

degradative ability under nonselective conditions, i.e., in the absence of the herbicide, is due to the deletion of the *rdpA* and *sdpA* genes. As two copies of IS*CR8* are located in the vicinity of these genes (Fig. 5) and additional copies are present on plasmid pMC1, deletion was previously hypothesized to be caused by homologous recombination between IS$CR8_L$ located upstream of *sdpA* and a copy of IS*CR8* presumed to be downstream of *rdpA* (15) (Fig. 5).

In this study, we sequenced the insert of cosmid R10 spanning the region downstream of *rdpA* and identified another IS*CR8* element. Furthermore, a copy of IS*1071* and part of the lower degradation pathway (*tfdRCD*), which is unaffected by the deletion events, were identified at the right end of cosmid insert R10. In PCR and Southern hybridization experiments (Fig. 5, PCR1 to 4 and Hyb1 to 3), IS$CR8_R$ was indeed found to mark the right border of the deletion. However, IS$CR8_L$ did not constitute the left end, the deleted region extended further to the left. We presume that recombination with another copy of IS*CR8* located in this region takes place during the deletion event. Attempts to clone and characterize this region failed due to the high instability of plasmid pMC1.

Conclusions. In this study IS*CR8*-like elements associated with degradative traits were analyzed with regard to structural features characteristic for functional IS*91* family insertion elements. Analysis revealed that besides IS*CR8* there are two more subgroups of IS*CR* elements, IS*CR22* and IS*CR23*. All three groups are defined and distinguished by the length and phylogenetic relationship of their transposases, the sequence of their *ori*IS, distance of the *ori*IS to the transposase ORFs, and the sequence of this intervening region. These results give strong evidence of IS*CR8/22/23* being functional and potentially active IS*CR* elements. The evolutionary success of IS*CR8/22/23* elements is highlighted by their very broad host range, their association with a wide variety of degradative traits, and their involvement in genetic rearrangements, potentially facilitating adaptive processes in their hosts.

To our current knowledge, the elements analyzed here are only marginally associated with antibiotic resistance. However, in principle any piece of DNA can be transferred by them, and the niches inhabited by IS*CR8/22/23* and those IS*CR* subgroups known to disseminate resistance determinants overlap (8, 9). The understanding of the IS*CR8/22/23* subgroup is therefore an important contribution to the understanding of the whole IS*CR* group of insertion elements. The common theme linking both sets of IS*CR* elements is their apparent usefulness for bacterial communities having to respond to recent challenges (e.g., antibiotics or xenobiotics).

ACKNOWLEDGMENTS

We gratefully acknowledge the excellent technical support of Ute Lohse and Anett Heidtmann.

K.M.S. was supported by Deutsche Bundesstiftung Umwelt (German Federal Environmental Foundation) grant 20000/99.

REFERENCES

1. **Altschul, S. F., W. Gish, W. Miller, E. W. Myers, and D. J. Lipman.** 1990. Basic local alignment search tool. J. Mol. Biol. **215:**403–410.
2. **Bernales, I., M. V. Mendiola, and F. de la Cruz.** 1999. Intramolecular transposition of insertion sequence IS*91* results in second-site simple insertions. Mol. Microbiol. **33:**223–234.
3. **Boerlin, P., and R. J. Reid-Smith.** 2008. Antimicrobial resistance: its emergence and transmission. Anim. Health Res. Rev. **9:**115–126.
4. **Chun, K. T., H. J. Edenberg, M. R. Kelley, and M. G. Goebl.** 1997. Rapid amplification of uncharacterized transposon-tagged DNA sequences from genomic DNA. Yeast **13:**233–240.
5. **Corpet, F.** 1988. Multiple sequence alignment with hierarchical clustering. Nucleic Acids Res. **16:**10881–10890.
6. **del Pilar Garcillan-Barcia, M., I. Bernales, M. V. Mendiola, and F. de la Cruz.** 2001. Single-stranded DNA intermediates in IS*91* rolling-circle transposition. Mol. Microbiol. **39:**494–501.
7. **Garcillan-Barcia, M. P., and F. Cruz.** 2002. Distribution of IS91 family insertion sequences in bacterial genomes: evolutionary implications. FEMS Microbiol. Ecol. **42:**303–313.
8. **Gordon, L., A. Cloeckaert, B. Doublet, S. Schwarz, A. Bouju-Albert, J. P. Ganiere, H. Le Bris, A. Le Fleche-Mateos, and E. Giraud.** 2008. Complete sequence of the floR-carrying multiresistance plasmid pAB5S9 from freshwater Aeromonas bestiarum. J. Antimicrob. Chemother. **62:**65–71.
9. **Heuer, H., C. Kopmann, C. T. Binh, E. M. Top, and K. Smalla.** 2009. Spreading antibiotic resistance through spread manure: characteristics of a novel plasmid type with low %G+C content. Environ. Microbiol. **11:**937–949.
10. **Kumar, S., K. Tamura, I. B. Jakobsen, and M. Nei.** 2001. MEGA2: molecular evolutionary genetics analysis software. Bioinformatics **17:**1244–1245.
11. **Ma, Y. F., J. F. Wu, S. Y. Wang, C. Y. Jiang, Y. Zhang, S. W. Qi, L. Liu, G. P. Zhao, and S. J. Liu.** 2007. Nucleotide sequence of plasmid pCNB1 from *Comamonas* strain CNB-1 reveals novel genetic organization and evolution for 4-chloronitrobenzene degradation. Appl. Environ. Microbiol. **73:**4477–4483.
12. **Mendiola, M. V., I. Bernales, and F. de la Cruz.** 1994. Differential roles of the transposon termini in IS*91* transposition. Proc. Natl. Acad. Sci. U. S. A. **91:**1922–1926.
13. **Mendiola, M. V., and F. de la Cruz.** 1989. Specificity of insertion of IS*91*, an insertion sequence present in alpha-haemolysin plasmids of Escherichia coli. Mol. Microbiol. **3:**979–984.
14. **Papanicolaou, G. A., A. A. Medeiros, and G. A. Jacoby.** 1990. Novel plasmid-mediated beta-lactamase (MIR-1) conferring resistance to oxyimino- and alpha-methoxy beta-lactams in clinical isolates of Klebsiella pneumoniae. Antimicrob. Agents Chemother. **34:**2200–2209.
15. **Schleinitz, K. M., S. Kleinsteuber, T. Vallaeys, and W. Babel.** 2004. Localization and characterization of two novel genes encoding stereospecific dioxygenases catalyzing 2(2,4-dichlorophenoxy)propionate cleavage in Delftia acidovorans MC1. Appl. Environ. Microbiol. **70:**5357–5365.
16. **Siguier, P., J. Perochon, L. Lestrade, J. Mahillon, and M. Chandler.** 2006. ISfinder: the reference centre for bacterial insertion sequences. Nucleic Acids Res. **34:**D32–D36.
17. **Sørensen, A. B., M. Duch, and F. S. Pedersen.** 1999. Isolation of unknown flanking DNA by a simple two-step polymerase chain reaction method. DYNA Logue **3**(99)**:**2–3.
18. **Tavakoli, N., A. Comanducci, H. M. Dodd, M. C. Lett, B. Albiger, and P. Bennett.** 2000. IS*1294*, a DNA element that transposes by RC transposition. Plasmid **44:**66–84.
19. **Thompson, J. D., T. J. Gibson, F. Plewniak, F. Jeanmougin, and D. G. Higgins.** 1997. The CLUSTAL_X windows interface: flexible strategies for multiple sequence alignment aided by quality analysis tools. Nucleic Acids Res. **25:**4876–4882.
20. **Toleman, M. A., P. M. Bennett, and T. R. Walsh.** 2006. Common regions e.g. orf513 and antibiotic resistance: IS91-like elements evolving complex class 1 integrons. J. Antimicrob. Chemother. **58:**1–6.
21. **Toleman, M. A., P. M. Bennett, and T. R. Walsh.** 2006. IS*CR* elements: novel gene-capturing systems of the 21st century? Microbiol. Mol. Biol. Rev. **70:** 296–316.
22. **Turner, S. A., S. N. Luck, H. Sakellaris, K. Rajakumar, and B. Adler.** 2001. Nested deletions of the SRL pathogenicity island of *Shigella flexneri* 2a. J. Bacteriol. **183:**5535–5543.
23. **Xu, D. Q., J. O. Cisar, N. Ambulos, Jr., D. H. Burr, and D. J. Kopecko.** 2002. Molecular cloning and characterization of genes for *Shigella sonnei* form I O polysaccharide: proposed biosynthetic pathway and stable expression in a live salmonella vaccine vector. Infect. Immun. **70:**4414–4423.
24. **Zaghloul, L., C. Tang, H. Y. Chin, E. J. Bek, R. Lan, and M. M. Tanaka.** 2007. The distribution of insertion sequences in the genome of *Shigella flexneri* strain 2457T. FEMS Microbiol. Lett. **277:**197–204.